Final Report for Period: 06/2011 - 05/2012
Submitted on: 02/12/2013
Principal Investigator: Fuller, Thomas F.
Award ID: 1118294
Organization: Georgia Tech Research Corp
Submitted By:
Fuller, Thomas - Principal Investigator
Title:
Long-term stability of Catalysts

Project Participants

Senior Personnel

Name: Fuller, Thomas
Worked for more than 160 Hours: Yes
Contribution to Project:

Post-doc

Graduate Student

Name: Gallagher, Kevin
Worked for more than 160 Hours: Yes
Contribution to Project:
Assisted new graduate student in getting started on the project. Developed complementary kinetic model of carbon oxidation, related to the stability of the catalyst system.

Name: Chandrasekaran, Raji
Worked for more than 160 Hours: Yes
Contribution to Project:
Assited new graduate student with experimental program.

Name: Setzler, Brian
Worked for more than 160 Hours: Yes
Contribution to Project:
New graduate student who started on program in Fall 2009. Literature reviews, learning experimental techniques, rudimentary modeling.

Name: George, Vyran
Worked for more than 160 Hours: No
Contribution to Project:
Outreach activities and measurement of transport properties

Undergraduate Student

Technician, Programmer

Other Participant

Research Experience for Undergraduates

Organizational Partners

Columbia University

Simon Billinge at Columbia University is one of the leading experts in the use of pair distribution function (PDF) testing.

Max-Planck-Institut f?r Festk?rperforsch
K. D. Kreuer is providing membrane sample for evalution of transport properties.

Argonne National Laboratory
Use of Advanced photon source at ANL for PDF measurements.

Brookhaven National Laboratory

Other Collaborators or Contacts

Activities and Findings

Research and Education Activities:
Three thrusts to the project: development of pair distribution methods for application to fuel cell catalysts, measurement of transport properties, modeling of platinum stability accounting for distribution of particle sizes.

Findings: (See PDF version submitted by PI at the end of the report)
see attached file

Training and Development:
The project has allowed students to developed capabilities in pdf (high energy x-ray) analysis. Additionally, they have learned physics based modeling of electrochemical systems.

Outreach Activities:
1. Instructor for KITES Science and Engineering Festival. Annual event at Scott Elementary School in Atlanta to expose underrepresented students to high quality science, technology, engineering and math (STEM) education.
2. Annual LEAD program for ENGINEERS? at GT. We led hands-on training in battery and fuel cells as part of 3-week Summer Engineering Institute for high school students from African American, Hispanic, and Native American communities.

Journal Publications

Gallagher, KG; Fuller, TF, "Kinetic model of the electrochemical oxidation of graphitic carbon in acidic environments", PHYSICAL CHEMISTRY CHEMICAL PHYSICS, p. 11557, vol. 11, (2009). Published, 10.1039/b915478

Gallagher, K.; Pivovar, B.; Fuller, T.F., "Electro-osmosis and Water Uptake in Polymer Electrolytes in Equilibrium with Water Vapor at Low Temperatures", Journal of the Electrochemical Society, p. B230, vol. 156, (2009). Published,

E. L. Redmond, B. P. Setzler, P. Juhas, S. J. L. Billinge, T. F. Fuller, "In-situ monitoring of particle growth at PEMFC cathode under accelerated cycling conditions", Electrochem. Solid-State Lett., p. B72, vol. 15, (2012). Published,

Trogodas, P; Fuller, T.F., "The effect of particle size distribution on Pt stability", ECS Transactions, p. 115, vol. 33(1), (2010). Published,

Fuller, TF, "Diagnostics for PEMFC Performance and Durability", ECS Transactions, p. 621, vol. 41 (1), (2011). Published,

Erin L. Redmond, Brian P. Setzler, Pavol Juhas, Simon J. L. Billinge, and T. F. Fuller, "Surface Energy Effects on Catalyst Degradation in Low-Temperature PEMFCs, Diagnostics for PEMFC Performance and Durability", ECS Transactions, p. 751, vol. 41 (1), (2011). Published,

Trogodas, P; Fuller, T.F., "The Effect of Uniform Particle Size Distribution on Pt Stability", ECS Transactions, p. 761, vol. 41 (1), (2011). Published,

E. L. Redmond, P. Trogadas, F. M. Alamgir, T. F. Fuller, "The effect of platinum oxide growth on platinum stability in PEMFCs", ECS Transactions, p. 1369, vol. 50 (2), (2012). Published,

Books or Other One-time Publications

Web/Internet Site

Other Specific Products

Contributions

Contributions within Discipline:

PDF has not been used for study of degradation of fuel cells. This opens up a new area for study.

The study of transport of Pt ions in ionomer membranes has the potential to significantly improve our understanding of pt dissolution.

Contributions to Other Disciplines:

Contributions to Human Resource Development:

Contributions to Resources for Research and Education:

Contributions Beyond Science and Engineering:

Conference Proceedings

Categories for which nothing is reported:

Any Book
Any Web/Internet Site
Any Product
Contributions: To Any Other Disciplines
Contributions: To Any Human Resource Development
Contributions: To Any Resources for Research and Education
Contributions: To Any Beyond Science and Engineering
Any Conference

Highlights Long-term stability of Catalysts PI Thomas F. Fuller

PDF methods

Techniques to measure the surface energy of solid nanoparticles are needed to better understand better the effects of this parameter on fuel- cell catalyst stability. Platinum nanoparticles are important in facilitating the oxygen reduction reaction that takes place at the cathode of proton exchange membrane (PEM) fuel cells. The marketability of PEM fuel cells for automotive applications is limited by the cost, which is increased by use of a platinum catalyst. One approach to minimize cost, while maintaining an acceptable level of performance, is the use of small, supported platinum nanoparticles ranging from 2 to 5 nm. However, high potentials and acidic conditions present at the cathode result in platinum instability, and electrochemically active surface area decreases over time. The loss of active catalyst area reduces fuel-cell efficiency. Platinum area loss occurs through two processes, nano-scale Ostwald ripening and micro-scale platinum deposition in the membrane, both of which are accelerated by small particle sizes. Ostwald ripening is a process driven by surface energy in which large particles grow at the expense of small particles. Pair distribution methods (PDF) have been applied to catalysts for fuel cells. These efforts resulted in new insights into the surface energy of nanoparticles and their effect on platinum stability.

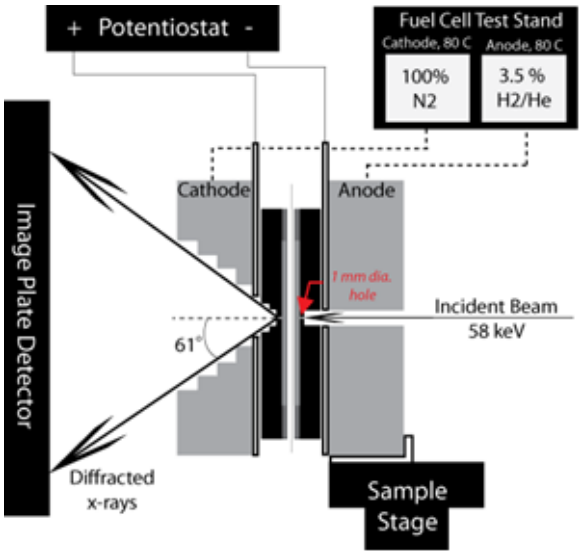

An in-situ method to measure changes in catalyst particle size at the cathode of a proton exchange membrane fuel cell was demonstrated. Synchrotron x-rays, 58 keV, were used to measure the pair distribution function on an operating fuel cell and observe the growth of catalyst particles under accelerated degradation conditions. The stability of Pt/C and PtCo/C with different initial particle sizes was monitored over 3000 potential cycles. The increase in particle size was fit to a linear trend as a function of cycles. The most stable electrocatalyst was found to be the alloyed PtCo with the larger initial particle size. This new method provides another tool to investigate platinum stability.

Electro-osmotic drag

Under this portion of the project we continued to explore the transport properties of novel ionomer membranes. It is believed that these transport properties are important for the challenge of platinum stability. For the first time, we found that for ionomer membranes other than Nafion, that the electro-osmotic drag coefficient was not unity. Because of the unique mechanisms for transport of protons compared to other ions, these results offer the possibility of tailoring the ionomers to maintain proton conductivity and hinder mobility of platinum ions.

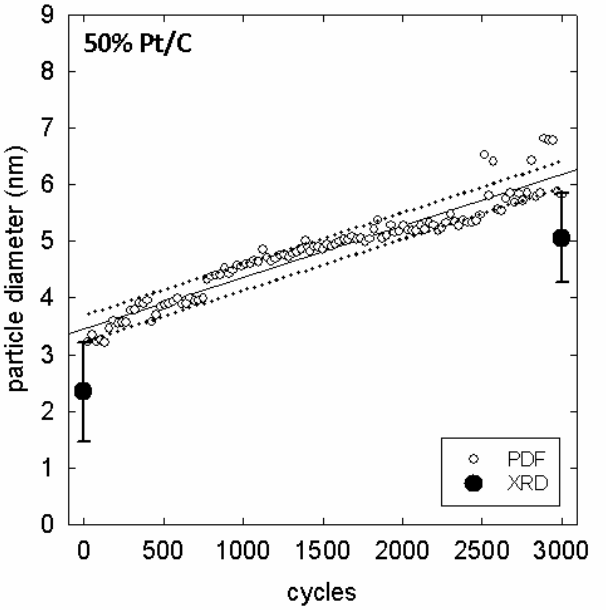

Modeling of Pt stability

Previous models of platinum stability have considered just two particle sizes. This work developed a macro-homogeneous model of platinum stability that included an arbitrary initial particle distribution of sizes. Using population balance methods, the model provides insight into the evolution of particles sizes during potential cycling. Typical results are shown in the figure to the right that illustrate the growth in particle size as well as the broadening of the distribution.

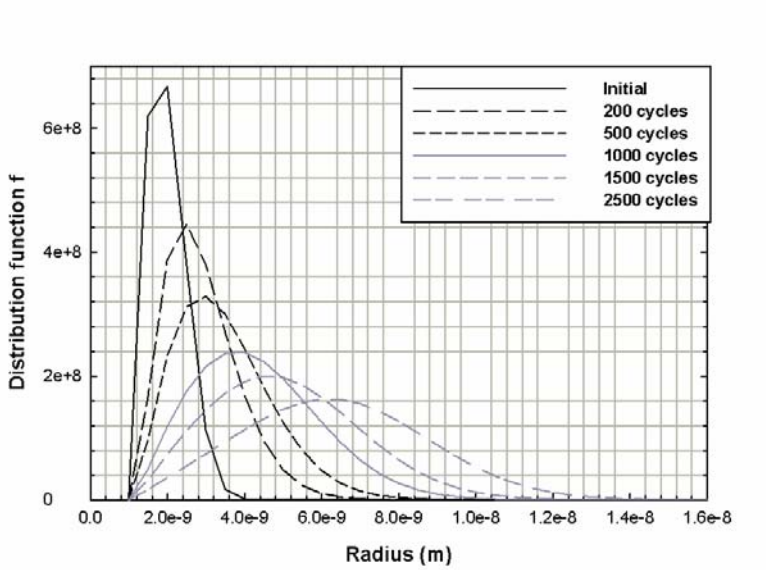

Publications

1. Kevin Gallagher, Bryan Pivovar, T. F. Fuller, Electro-osmosis and Water Uptake in Polymer Electrolytes in Equilibrium with Water Vapor at Low Temperatures*, J. Electrochem. Soc.*, **156**, B330-B338 (2009).
2. P. Trogadas, T. F. Fuller, The effect of particle size distribution on Pt stability, *ECS Trans.*, **33** (1), 115-124 (2010).
3. T. F. Fuller, Diagnostics for PEMFC Performance and Durability, *ECS Trans*., **41** (1), 621 (2011).
4. Erin L. Redmond, Brian P. Setzler, Pavol Juhas, Simon J. L. Billinge, and T. F. Fuller, Surface Energy Effects on Catalyst Degradation in Low-Temperature PEMFCs, Diagnostics for PEMFC Performance and Durability, *ECS Trans*., **41** (1), 751 (2011).
5. P. Trogadas, T. F. Fuller, The Effect of Uniform Particle Size Distribution on Pt Stability, *ECS Trans*., **41** (1), 761 (2011).
6. E. L. Redmond, B. P. Setzler, P. Juhas, S. J. L. Billinge, T. F. Fuller, In-situ monitoring of particle growth at PEMFC cathode under accelerated cycling conditions, *Electrochem. Solid-State Lett*., **15**, B72-B74 (2012).
7. E. L. Redmond, P. Trogadas, F. M. Alamgir, T. F. Fuller, The effect of platinum oxide growth on platinum stability in PEMFCs, *ECS Trans*., **50** (2) 1369-1376 (2012).

Presentations

1. Role of particle size distribution on Pt stability, (P. Trogadas speaker), 218th Meeting of the Electrochemical Society, Las Vegas, October, 2010.
2. Durability of Electrochemical Systems for Energy Conversion and Storage: Stability of Catalyst Systems, invited speaker Department of Materials Science and Chemical Engineering, Shizuoka University, Hamamatsu, Japan. July 28, 2011.
3. Diagnostics for PEMFC Performance and Durability, (invited talk) 220th Meeting of the Electrochemical Society, Boston, October, 2011.
4. Surface energy effects on catalyst degradation in low-temperature PEMFCs, Erin L. Redmond (speaker), Brian P. Setzler, Amir Matz, Pavol Juhas, Simon J.L. Billinge, 220th Meeting of the Electrochemical Society, Boston, October, 2011.
5. GT Center for Innovative Fuel Cell and Battery Technologies, US-Taiwan Workshop on Energy Storage, sponsored by NSF, Minneapolis, MN. October 15, 2011.

6. Determination of Electroosmotic Drag and Proton Conduction Mechanism In Proton Exchange Membranes for Use In Low Temperature PEMFCs, (Brian P. Setzler speaker) AIChE Annual Meeting, Minneapolis, MN. October 18, 2011.
7. "The effect of Platinum Oxide Growth on Platinum Stability in PEMFCs," Erin L. Redmond (speaker), Panagiotis Trogadas, Faisal M. Alamgir, and Thomas F. Fuller, 222nd Meeting of the Electrochemical Society, Honolulu, October, 2012.

Outreach

1. Instructor for KITES Science and Engineering Festival. Annual event at Scott Elementary School in Atlanta to expose underrepresented students to high quality science, technology, engineering and math (STEM) education.
2. Annual LEAD program for ENGINEERS® at GT. We led hands-on training in battery and fuel cells as part of 3-week Summer Engineering Institute for high school students from African American, Hispanic, and Native American communities.

Particle Size Distribution Effects on Platinum Dissolution

The instability of Pt electrocatalysts under operating fuel-cell conditions is one of the main barriers towards commercialization of polymer electrolyte fuel cells (PEFC). PEFCs operating under potential cycling conditions gradually lose the electrochemically active surface area (ECA) of the cathode due to nanoparticle dissolution and growth.[1]

The loss of area is caused by Ostwald ripening at potentials higher than 0.8 V (vs standard hydrogen electrode; SHE)[2] where large Pt particles grow at the expense of small ones via interparticle transport of single atoms[1b,2c,3] or carbon support corrosion (at potentials greater than 1.1V (SHE)[4] leading to the detachment and agglomeration of Pt nanoparticles. [3b]

Detailed numerical models on Pt oxidation were reported by Darling and Meyers.[3f-g] Empirical Butler-Volmer equations were used to calculate the platinum/carbon oxide coverage without taking into account the intermediate species of oxygen reduction reaction (ORR) and water adsorption on catalyst surface. It was reported that Pt dissolution in PEFCs is large at potentials above 0.9 V (SHE).[3g]

Shao-Horn and coworkers[5] constructed a thermodynamic-kinetic model and simulated ex-situ (assuming zero hydrogen crossover and Pt diffusion from the cathode) and in-situ (assuming Pt diffusion from the anode and presence of hydrogen crossover) experimental conditions. It was predicted that in the ex-situ experimental environment, Pt surface area loss and particle size distribution was dominated by coarsening. In the simulated in-situ environment, crossover hydrogen increased the Pt mass flow from the particle surface resulting to an increase of Pt surface area loss. Simulations have demonstrated that Pt stability was improved once the Pt particle size was increased from 2 to 5 nm (in-situ experimental conditions), although the effect of particle size enhancement on electrochemically active surface area or Pt activity was not taken into account.

The effect of hydrogen crossover in Pt reduction was demonstrated in the models developed by Fuller's group.[3e, 6] A Pt band is formed in the ionomer during Pt precipitation reaction and a model based on gas crossover rates (H_2 and O_2) was constructed to predict its location.[3e] The calculated band position was similar to the experimental position detected with scanning electron microscopy (SEM).[3e] The effect of reactant gas partial pressure and relative humidity (RH) on Pt dissolution was also investigated.[6a] Reactant gas partial pressure did not alter the rate of cathode degradation,[6a] whereas an increase in RH resulted in higher Pt degradation rates leading to an approximate two- and three-fold reduction of ECA and cathode Pt mass respectively at 100%RH (compared to 50% RH).[6a] Cathode catalyst degradation was modeled using a bi-modal particle-size distribution[6b] refining Darling-Meyers models[3f-g] and Pt particle growth was revealed through mass exchange of Pt between small and large particles.

Despite previous modeling efforts[3e-g,5,6a-b,7], the effect of uniform particle size distribution (PSD) on Pt stability under potential cycling is still unknown. It is expected that Pt stability will be improved if narrow PSDs are used, the high cost of these distributions and the difficulty of their fabrication notwithstanding. The present study aims to address this effect by building a theoretical model based on the chemical reactions of Pt oxidation and precipitation in the membrane. The incorporation of an arbitrary function for the initial PSD and a population balance[8] allows the investigation of the effect of PSD on degradation. Both the evolution of the PSD and the Pt ion concentration in the ionomer can be monitored with time.

Pt Dissolution Model

The domain modeled (Fig. 1) consists of two regions joined by an interface. The electrode region represents the Pt/C electrocatalyst (thickness L_1) on the cathode side of the membrane electrode assembly (MEA) while the membrane region represents the part of the polymer electrolyte (thickness L_2) up until the point where the Pt band is formed.[3e] The potential of the electrode is cycled as a function of time between 0.5 and 1 V (vs. SHE) and with a period of 30 s.

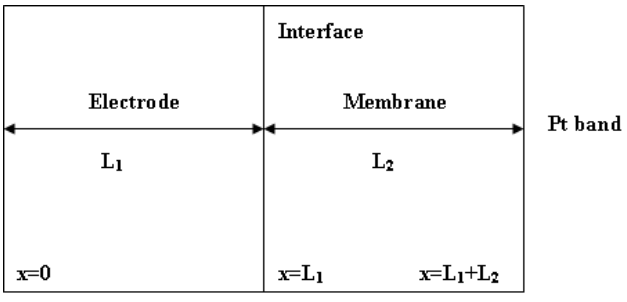

Figure 1. Pt dissolution model.

The main model assumptions are the following

1. One dimensional, macroscopic model. Since the MEA thickness (6 μm anode/cathode and 20μm PEM) is much smaller than the

in-plane dimensions (5-30 cm) of the MEA, a 1D approach is valid. In-plane uniformity is assumed.

2. Pt/C solid phase is uniformly mixed with Nafion® electrolyte and gas pore phase in the cathode forming a porous electrode. Polymer volume fractions (ε) are assumed to be one in PEM separator and 0.30 in the cathode based on the experimental porosity values reported for Nafion®-based electrodes varying between ~ 0.2 and ~ 0.4 as a function of their solvent composition.[9]
3. Pt particles are initially uniformly distributed through the thickness of the cathode. A platinum loading of 0.5 mg cm^{-2} is considered for the calculation of the number density of particles in the catalyst layer, representing a typical value for an MEA.
4. Pt ions are transported by diffusion into the PEM, and they are reduced by crossover hydrogen forming a Pt band in the membrane. The width of Pt band is neglected and Pt ion concentration at the band is equal to zero.

The Platinum degradation mechanism is described by two electrochemical reactions, namely Pt electrochemical dissolution (~ 1.2V vs. SHE; reaction R1) within the electrode (Fig. 1) and Pt precipitation by hydrogen reduction at the Pt band in the membrane (Fig. 1). Because our interest here is to explore the effect of initial PSD on degradation, and because the kinetics are unknown, platinum oxide chemical dissolution is not considered.[3g]

A modified Butler-Volmer equation[3g,6b] is used in the electrode region to describe the reaction rate. A finite rate of mass transfer is assumed, and the equilibrium potential is shifted with the Kelvin equation to account for the dependence on particle size and size distribution.

$$Pt \leftrightarrow Pt^{2+} + 2e^- \qquad (R1)$$

$$\frac{i_1}{nF} = k_1\left[\exp\left(\frac{a_a nF(E-U_1)}{RT}\right) - \frac{c}{c^o}\left(\exp\left(\frac{-a_c nF(E-U_1)}{RT}\right)\right)\right] \qquad (2)$$

For small, spherical particles the slip velocity is assumed to be negligible and the Sherwood number is two. Thus, the mass transfer coefficient is expressed as[3c]

$$k_c = \frac{D}{R} \qquad (3)$$

As a result, the reaction rate i_1 / nF including a mass-transfer resistance is

$$\frac{i_1}{nF} = \frac{k_1\left[\exp\left(\frac{\alpha_a nF(E-U_1)}{RT}\right) - \frac{c}{c^o}\exp\left(\frac{-\alpha_c nF(E-U_1)}{RT}\right)\right]}{1 + \frac{\exp\left(\frac{-\alpha_c nF(E-U_1)}{RT}\right)\cdot r}{2\cdot D\cdot c^o}} \qquad (4)$$

where the thermodynamic potential U_1 is given by the following equation

$$U_1 = U_1^0 - \frac{\gamma \cdot MW}{\rho \cdot r} \qquad (5)$$

The second term on the right side shows the effect of the surface energy of the platinum crystallite on the equilibrium potential; as the platinum particle shrinks, the shift in chemical potential of Pt increases.[3g]

A modified Butler-Volmer equation is also used to describe the Pt oxidation reaction rate

$$Pt + H_2O \leftrightarrow PtO + 2H^+ + 2e^- \qquad (R2)$$

The anodic term represents the formation of PtO, and the cathodic term describes the reduction of PtO to Pt.

$$\frac{i_2}{nF} = k_2\left[\exp\left\{\frac{-\omega\theta}{RT}\right\}\exp\left\{\frac{a_a nF(E-U_2)}{RT}\right\} - C_H^2\,\theta\exp\left\{\frac{-a_c nF(E-U_2)}{RT}\right\}\right] \qquad (6)$$

where the thermodynamic potential U_2 is given by the following equation

$$U_2 = U_2^0 + \frac{1}{2F}\left(\Delta\mu_{PtO}^o + \frac{\sigma_{PtO} MW_{PtO}}{\rho_{PtO} r} - \frac{\sigma \cdot MW}{\rho \cdot r}\right) \qquad (7)$$

The initial number density of Pt particles, N, is calculated to achieve the desired Pt loading. N depends on the initial particle size distribution, $f(r)$. Assuming spherical particles,

$$\int_0^{L_1}\int_0^{\infty} N\rho_{Pt} f(r)\frac{4}{3}\pi r^3 dr dx = 0.005\ \mathrm{kg\ m^{-2}} \qquad (8)$$

For a Gaussian distribution (σ=0.3, r_o=2nm)

$$N = 6\cdot 10^{22}\ m^{-3} \qquad (9)$$

A mass balance on platinum in a differential control volume in the cathode is needed. Pt can either be in the solution as platinum ions or deposited as Pt metal in the solid phase. This material balance is given by equation (10). The diffusion coefficient in

the porous electrode is corrected for porosity and tortuosity ($\tau = \varepsilon^{-0.5}$).

$$\varepsilon \frac{\partial c}{\partial t} = D \frac{\varepsilon}{\tau} \frac{\partial^2 c}{\partial x^2} + \int_0^{\infty} f(r) \cdot \frac{i_1}{nF} \cdot N \cdot 4\pi \cdot r^2 \cdot dr \qquad (10)$$

The term on the left represents the time rate of change of Pt^{2+} in the electrolyte, the first term on the right side is the net efflux of Pt ions from diffusion. The last term on the right side is the rate of change of the total amount of solid Pt present in the control volume. This term can also be thought of as a homogeneous reaction rate for dissolution or precipitation.

Boundary and initial conditions for equation (10) are

$$\frac{\partial c}{\partial x}(x = 0) = 0 \qquad (11)$$

$$c(x = L) = 0 \qquad (12)$$

$$c(x, t = 0) = c^o \qquad (13)$$

A population balance is used to follow the change of the PSD function $f(r)$ over time[8]

$$\frac{\partial f(r)}{\partial t} = \frac{MW}{\rho} \frac{\partial \left(\frac{i_1}{nF} \cdot f(r) \right)}{\partial r} \qquad (14)$$

Selection of the initial particle distribution $f(r,t=0)$ is governed by the functional form that best fits the experimentally measured PSD of the solids being studied. Three distribution functions commonly used for modeling ground solids are the Gaussian, log normal, and Schulz distribution.[8,10] The Gaussian distribution (Table 1) was chosen because it allows for the most straightforward analysis of the effect of PSD. With the Gaussian distribution the initial particle radius (r_o) and mean standard deviation (σ; width of particle distribution) can be varied independently, conversely it is difficult to make the same comparisons using log-normal or Schulz distributions.

Table 1. Particle size distributions tested.

Distribution	f(r,t=0)
Gaussian	$f(r, t = 0) = \frac{1}{r_o \cdot \sigma \cdot \sqrt{2 \cdot \pi}} \exp\left\{ \frac{-\left(\frac{r}{r_o} - 1 \right)^2}{2 \cdot \sigma^2} \right\}$

At the boundary, a platinum band is formed via hydrogen reduction (reaction R3).

$$Pt^{2+} + H_2 \leftrightarrow Pt + 2H^+ \qquad (R3)$$

In the membrane region, there is no homogeneous reaction, and equation (10) reduces to Fick's second law. The same initial and boundary conditions following auxiliary conditions are used.

The distribution of Pt concentration in the cathode catalyst layer was determined numerically with gPROMS®. The model equations were integrated in the software and solved using the central finite difference equation.

Results and Discussion

The superficial current density, I, is the sum of contributions from all particle sizes, and the current density normal to the surface of the porous electrode integrated over its thickness,

$$I = \int_0^{L_1} \int_0^{\infty} 4 \cdot \pi \cdot r^2 \cdot N \cdot f(r) \cdot (i_1 + i_2) \cdot dx \cdot dr \qquad (15)$$

Figure 2 shows the simulated and measured fuel-cell cathode cyclic voltammetry (CV) curves at 60 °C and fully humidified conditions with a sweep rate of 50 mV s^{-1} from 0.6 to 1 V (vs. SHE). Hydrogen adsorption and desorption (at potentials lower than 0.4 V vs. SHE) were not simulated. The shape of CV curve was not affected by Pt dissolution currents as their value was always two to three orders of magnitude lower than Pt oxidation currents. The simulated CV does not provide a good fit to the experimental curve since the predicted and experimental reduction peaks have different shapes, indicating that the particles of the model discharge at a higher potential than what it is observed experimentally. A revised physical model is needed to improve the CV fit to experimental data which is the subject of a future work. Nevertheless, the effect of PSD can be investigated with this model. Table 2 lists the model parameters. The fitted Pt oxidation reaction rate constant (k_2) was higher than the values reported in the literature due to the different PSDs, experimental conditions and nature of Pt electrode. The rest of the fitted parameters were close to the literature values.

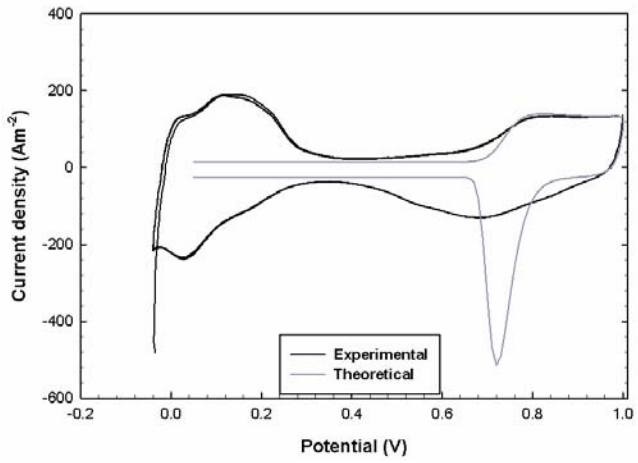

Figure 2. Experimental and theoretical cyclic voltammograms.

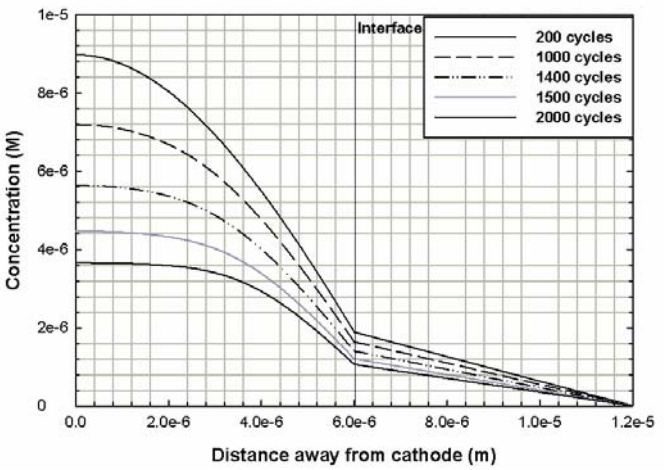

Figure 3. Pt^{2+} concentration as a function of distance away from cathode at E = 1 V vs. SHE (r_o = 2 nm, σ = 0.3).

Table 2. Fitted parameters.

Variables	Fitted values	Literature values
D	$1\cdot10^{-10}$ m^2s^{-1}	$1\cdot10^{-10}$-$1.5\cdot10^{-13}$ m^2s^{-1} [3g,8b]
k_1	$1\cdot10^{-5}$ $molm^{-2}s^{-1}$	$3.4\cdot10^{-9}$$molm^{-2}s^{-1}$ [3g]
k_2	$1\cdot10^{-6}$ $molm^{-2}s^{-1}$	$1\cdot10^{-9}$-$1\cdot10^{-14}$$molm^{-2}s^{-1}$[13]

The initial testing of the model involved potential sweep simulations (between 0.5 and 1 V vs. standard hydrogen electrode (SHE), 30 sec period). It was assumed that electrode and membrane had the same thickness (6 μm each), while the adopted initial platinum concentration value was 10^{-9} M. Figure 3 represents Pt^{2+} concentration as a function of the distance from the back of the cathode during potential sweeps between 0.5 and 1 V. As the particles grow in size, the equilibrium concentration of Pt^{2+} for a fixed potential decreases. Therefore, concentration values are slowly reduced with increasing cycles due to the growth of average particle size. Different porosity values have been used for the electrode and membrane (ε=0.3 and 1 respectively) resulting in different slopes in these two regions.

Figure 4 represents the evolution of the Pt PSD in the electrode (x = 0) under potential cycling. An initial Gaussian particle distribution was used assuming that the geometric mean diameter (r_o) was 2 nm and the standard deviation (σ) was 0.3. The area under these curves is equal to the fraction of the total number of particles present at any time. It is demonstrated that the distribution shifts towards larger diameters and broadens as a function of time; this phenomenon is a result of both a loss in mass of the particles (preferentially for smaller particles) and the growth of large particles at the expense of small and medium particles (Ostwald ripening).[1b,3a-c]

Furthermore, it was revealed that the size distributions of spherical platinum particles were similar across the cathode thickness. This observation is consistent with previous reports in the literature.[1b,11a] Cross-sectional analysis of aged PEFC[1b] and PAFC[11a] cathodes demonstrated the independence of particle size as a function of cathode thickness. Thus, it can be stated that the coarsening of spherical platinum particles on carbon across the cycled MEA cathode thickness proceeds under Ostwald ripening. As it is driven by the reduction of the surface energy of platinum particles, small particles disappear and the PSD shifts towards larger values in the cycled cathode compared to the pristine sample (Figure 4).

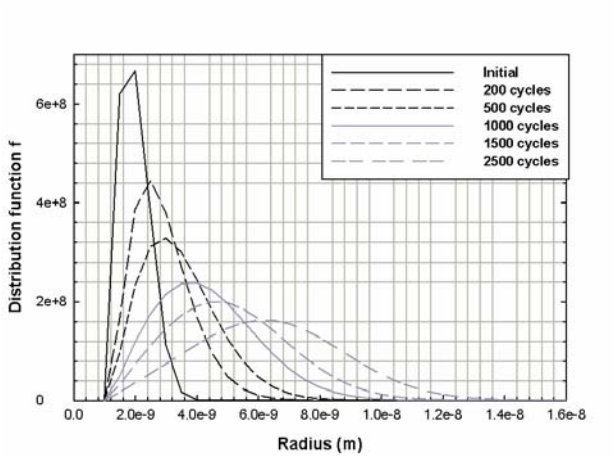

Figure 4. Particle size distribution in the electrode (x = 0) during potential cycling (r_o = 2 nm, σ = 0.3).

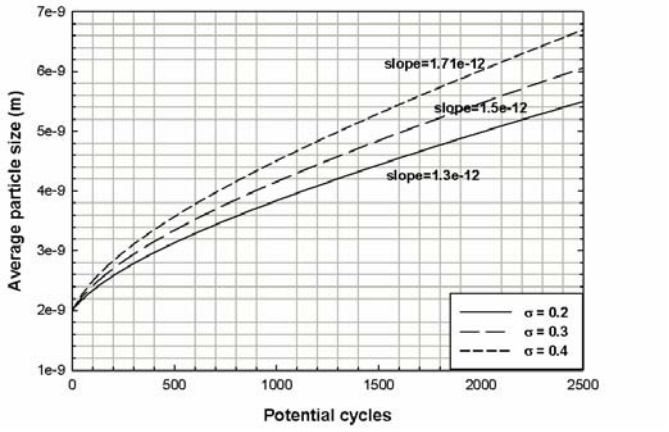

Figure 5. Particle size growth in the electrode (x=0) of narrower / wider distributions.

The n^{th} moment of a distribution function is defined as

$$n^{th}\ \text{moment} = \mathrm{M_n} = \int_0^\infty f(r)\cdot r^n \cdot dr \qquad (15)$$

The first four moments have the following physical significances [11b]: number of particles, average particle size, area of particles or ECA, and volume or amount of Pt mass.

The reduction in ECA and loss of Pt mass increased as the initial PSD was broadened. As shown in Table 3, the ECA and Pt mass were reduced by 19% and 17% for σ = 0.4. In contrast, for a more narrow distribution (σ = 0.2) the reductions were 9% and 7% respectively. In order to keep the loading constant, the number density, N changed with σ. The effect of the width of the initial PSD (σ) on average particle size was also investigated. Plots of average particle size versus potential cycles were constructed (Figure 5), and it was revealed that initial rapid increase in size is caused by the rapid dissolution of the smallest particles (tail of PSD). These small particles are not stable even at low potentials. More important is the slope of the particle growth after the rapid early-stage growth; the slope becomes steeper towards wider particle size distributions. The slope of the curve can also be directly related to the particle growth rate, demonstrating that the narrower the distribution the more stable it is.

Table 3. Calculated ECA and Pt mass loss for PSDs of varying width (r_o = 2 nm, σ = 0.3).

	ECA loss	Mass loss
σ = 0.2	9%	7%
σ = 0.3	15%	13%
σ = 0.4	19%	17%

Model validation

Reasonable correlations exist between model predictions and experimental ECA loss studies conducted at 0.95 and 0.75 V (vs. SHE).[1b] Table 4 shows the comparison between model calculations and ECA loss experiments at constant potentials; predicted and measured ECA loss at 0.95 V (vs. SHE) are similar while there is a 15% variation in the predicted ECA loss data at 0.75 V (vs. SHE), which can be ascribed to the elimination of particle agglomeration / redeposition processes in the model.

Table 4. Comparison of predicted ECA loss with experimental data (r_o = 2 nm, σ = 0.3).[1b]

	ECA loss (0.95 V vs. SHE)	ECA loss (0.75 V vs. SHE)
Experiment[1b]	80%	40%
Model	85%	29%

Additionally, particle growth follows an almost linear increase as a function of potential cycles, which is in agreement with in-situ high energy x-ray results (Figure 6).[12]

However, further refinements are needed to describe more accurately the Pt degradation behavior including: *i)* the incorporation of additional catalyst degradation mechanisms to the model such as Pt cluster formation on carbon support as well as Pt agglomeration / redeposition; *ii)* a detailed Pt oxide growth mechanism taking into account the interfacial place exchange step of

PtO to OPt that results in the creation of a surface lattice with Pt^{2+} and O^{2-} moieties[13]; and *iii)* the use of an additional transport equation to better describe the effect of Pt ions on catalyst pores as well as the introduction of a surface energy term that is dependent on particle radius. These refinements are needed to describe more accurately cathode degradation behavior over typical lifetimes of PEFCs.

In conclusion, a theoretical model was built to examine the effect of uniform Pt particle size distribution on Pt stability. A modified Butler-Volmer equation was used in the electrode region to describe the reaction rate taking into account the size dependency of particle stability and particle size distribution; a mass balance of platinum in the cathode and a population balance to monitor the change of particle size distribution function were also used. Potential cycling simulation (0.5 to 1 V vs. SHE; 30 sec period; 2000 cycles) demonstrated that Pt^{2+} concentration was slowly reduced due to the increase of average particle size while particle size distribution shifted towards larger diameters as a function of time. Calculation of the first four moments of particle size distribution demonstrated that as the PSD shifts towards wider distributions, the ECA and Pt mass loss rates are increasing as well, revealing that the uniformity of PSD plays an important role on Pt stability. The proposed model is one of the first physics based models that quantified the effect of the uniformity of PSD on catalyst degradation rate and this information can be used for the design of new catalysts for fuel cell applications.

[1] a) J. Xie, D. L. Wood, D. W. Wayne, T. A. Zawodzinski, P. Atanassov, R. L. Borup, *J. Electrochem. Soc.* **2005**, *152*, A104-A113; b) P. J. Ferreira, G. J. la O', Y. Shao-Horn, D. Morgan, R. Makharia, S. Kocha, H. A. Gasteiger, *J. Electrochem. Soc.* **2005**, *152*, A2256-A2271; c) C. A. Reiser, L. Bregoli, T. W. Patterson, J. S. Yi, J. D. Yang, M. L. Perry, T. D. Jarvi, *Electrochem. Solid-State Lett.* **2005**, *8*, A273-A276; d) P. Yu, M. Pemberton, P. Plasse, *J. Power Sources* **2005**, *144*, 11-20.

[2] a) P. Bindra, S. J. Clouser, E. Yeager, *J. Electrochem. Soc.* **1979**, *126*, 1631-1632; b) H. Honji, T. Mori, K. Tamura, Y. Hishinuma, *J. Electrochem. Soc.* **1988**, *135*, 355-359; c) X. Wang, R. Kumar, D. J. Myers, *Electrochem. Solid-State Lett.* **2006**, *9*, A225-A227.

[3] a) C. G. Granqvist, R. A. Buhrman, *J. Catal.* **1976**, *42*, 477-479; b) Y. Shao-Horn, W. C. Sheng, S. Chen, P. J. Ferreira, E. F. Holby, D. Morgan, *Top. Catal.* **2007**, *46*, 285-305; c) I. M. Lifshitz, V. V. Slyozov, *J. Phys. Chem. Solids* **1965**, *19*, 35-50; d) S. C. Ball, S. L. Hudson, D. Thompsett, B. Theobald, *J. Power Sources* **2007**, *171*, 18-25; e) W. Bi, G. E. Gray, T. F. Fuller, *Electrochem. Solid-State Lett.* **2007**, *10*, B101-B104; f) J. P. Meyers, R. M. Darling, *J. Electrochem. Soc.* **2006**, *153*, A1432-A1442; g) R. M. Darling, J. P. Meyers, *J. Electrochem. Soc.* **2003**, *150*, A1523-A1527; h) Y. Shao, G. Yin, Y. Gao, *J. Power Sources* **2007**, *171*, 558-566; i) A. V. Virkar, Y. Zhou, *J. Electrochem. Soc.* **2007**, *154*, B540-B547; k) J. Zhang, B. A. Litteer, W. Gu, H. Liu, H. A. Gasteiger, *J. Electrochem. Soc.* **2007**, *154*, B1006-B1011.

[4] D. A. Stevens, M. T. Hicks, G. M. Haugen, J. R. Dahn, *J. Electrochem. Soc.* **2005**, *152*, A2309-A2315.

[5] E. F. Holby, W. Sheng, Y. Shao-Horn, D. Morgan, *Energy Environ. Sci.* **2009**, *2*, 865-871.

[6] a) W. Bi, Q. Suna, Y. Deng, T. F. Fuller, *Electrochim. Acta* **2009**, *54*, 1826-1833; b) W. Bi, T. F. Fuller, *J. Power Sources* **2008**, *178*, 188-196.

[7] a) G. C. Allen, P. M. Tucker, A. Capon, R. Parsons, *J. Electroanal. Chem.* **1974**, *50*, 335-343; b) J. S. Hammond, N. Winograd, *J. Electroanal. Chem.* **1977**, *78*, 55-69; c) K. Kinoshita, J. T. Lundquist, P. Stonehart, *J. Electroanal. Chem. Int. Electrochem.* **1973**, *48*, 157-166.

[8] S. E. LeBlanc, H. S. Fogler, *AICHE J.* **1987**, *33*, 54-63.

[9] J. P. G. Villaluenga, V. M. Barragan, B. Seoane, C. Ruiz-Bauza, *Electrochim. Acta* **2006**, *51*, 6297-6303.

[10] S. R. Aragon, R. Pecora, *J. Chem. Phys.* **1976**, *64*, 2395-2404; M. Kotlarchyk, S. H. Chen, *J. Chem. Phys.* **1983**, *79*, 2461-2469.

[11] a) J. Aragane, T. Murahashi, T. Odaka, *J. Electrochem. Soc.* **1988**, *135*,844-850.; b) M. H. DeGroot, M. J. Schervish, in *Probability and Statistics*, 4th ed., Addison-Wesley, Boston, **2011**, *Ch. 5*, pp 302-306.

[12] E. L. Redmond, B. P. Setzler, P. Juhas, S. J. L. Billinge, T. F. Fuller, *Electrochem. Solid-State Lett.* **15,** B72-B74 (2012).

[13] G. Jerkiewicz, G. Vatankhah, J. Lessard, M. P. Soriaga, Y. S. Park, *Electrochim. Acta* **2004**, *49*, 1451-1459.